Polarization Independent Optical Coherence Tomography

Asha Parmar, Gargi Sharma, and Kanwarpal Singh

***Abstract*—Optical coherence tomography (OCT) is a well established imaging modality for high-resolution three-dimensional imaging in clinical settings. While imaging, care must be taken to minimize the imaging artifacts related to the polarization differences between the sample and the reference signals. Current OCT systems adopt complicated mechanisms, such as the use of multiple detectors, polarization-maintaining fibers, polarization controllers to achieve polarization artifacts free sample images. Often the polarization controllers need readjustment which is not suitable for clinical settings. In this work, we demonstrate a simple approach that can minimize the polarization-related artifacts in the OCT systems. Polarization artifact-free images are acquired using two orthogonally polarized reference signals where the orthogonal polarization is achieved using a Faraday mirror. In the current approach, only a single detector is required which makes the current approach compatible with swept-source or camera-based OCT systems. Furthermore, no polarization controllers are used in the system which increases the system stability while minimizing the artifacts related to the sample birefringence, polarization change due to the sample scattering, and polarization change due to the optical fiber movements present in the system.**

***Index Terms*—Optical coherence tomography, biomedical optical imaging, polarization artifacts, birefringence.**

I. Introduction

OPTICAL coherence tomography (OCT) [1] is a well-established tool for non-invasive, high-resolution, cross-sectional, three-dimensional imaging of biological samples. Based on low coherence interferometry [1]–[4], this technique measures the optical path difference between the optical signals reflected from the reference and the sample surface under investigation. Conventionally, OCT systems can broadly be divided into two categories, i.e., time-domain [1], [5], [6] and Fourier-domain OCT systems [7], [8]. In time-domain OCT systems, the reference mirror is translated axially to match the optical path difference between the reference surface and different layers of the sample, making this technique slow. The Fourier domain OCT systems overcame the limitation of the slow scan speed by either using a spectral-domain OCT (SD-OCT) approach where a broadband light source is used to image the sample in-depth and the interfered signal is detected using a spectrometer, or by sweeping the wavelength of a laser and measuring the interference signal using photodetectors in swept-source OCT (SS-OCT) [9], [10]. Both of these techniques are extensively used in clinical [11]–[16] and industrial applications [4], [17]–[19]. One of the primary requirements for the two signals to interfere is that their polarization should be the same. If there is any change in polarization because of the birefringence of the sample or because of bending and stretching of the fibers used in the system, it will result in imaging artifacts. The image quality will be reduced by a false enhancement in contrast or loss in signal in certain areas. To minimize these polarization artifacts in Fourier domain OCT, several techniques such as polarization-sensitive OCT (PS-OCT), cross-polarized OCT (CP-OCT), polarization diverse detection and optical switching have been proposed.

For instance, in PS-OCT systems [20]–[22], two images of the sample for electromagnetic field oscillating in two mutually orthogonal planes are acquired. PS-OCT allows one to get the information of retardance as well as the optic axis of the sample. The acquired images can be combined to eliminate the polarization-dependent artifacts. Similarly, CP-OCT systems [23]–[27], acquire two images of the sample, one for which the signal reflected from the sample has the same polarization as the illumination polarization and another for which the reflected signal polarization is orthogonal. Unlike PS-OCT which requires circular polarization for the sample illumination, the polarization of the sample illumination in CP-OCT can be any [24], [28], [29].

The polarization artifacts can also be minimized using a polarization-diverse detection unit [30], [31], where the orthogonally polarized interfered signal from the sample and the reference arm are detected and combined to reconstruct a polarization-independent image. Polarization-diverse detection unit scheme requires multiple detectors and hence is difficult to implement for spectrometer-based SD-OCT systems. Multiple cameras have been used in the PS-OCT system [3] to acquire two orthogonally polarized images simultaneously, but spectral matching for multiple cameras is extremely challenging.

The polarization artifacts in OCT have also been minimized using optical switching unit and synchronously detecting two orthogonally polarized images on a single spectrometer [32]. However, since the images are acquired sequentially, the sample

Manuscript received December 22, 2021; revised January 19, 2022; accepted January 30, 2022. Date of publication February 4, 2022; date of current version March 4, 2022. This work was supported by the Max Planck Society for the Advancement of Science. *(Corresponding author: Kanwarpal Singh.)*

Asha Parmar and Kanwarpal Singh are with the Max Planck Institute for the Science of Light, 91058 Erlangen, Germanyand also with the Department of Physics, Friedrich-Alexander-Universität Erlangen-Nürnberg, 91058 Erlangen, Germany (e-mail: asha.asha@mpl.mpg.de; kanwarpal.singh@mpl.mpg.de).

Gargi Sharma is with the Max Planck Institute for the Science of Light, 91058 Erlangen, Germany (e-mail: gargi.sharma@mpl.mpg.de).

This work involved human subjects or animals in its research. The author(s) confirm(s) that all human/animal subject research procedures and protocols are exempts from review board approval.

Digital Object Identifier 10.1109/JPHOT.2022.3148721

motion during the image acquisition can deteriorate the image quality. Furthermore, the use of an optical switch reduces the imaging speed by half.

In this work, we demonstrate a simple polarization-insensitive OCT system based on the use of two orthogonally polarized reference signals where the orthogonal polarization is achieved using a Faraday mirror. Our design compensates completely the polarization artifacts without the need for any active polarization controller and therefore will be suitable for clinical applications.

II. Methods

In a standard OCT system, for a homogenous sample without any birefringence, the amplitude of the recorded interference spectrum by the detector can be represented as [22]

$$A(\Delta z) = A_0(\Delta z)\cos[\phi(\Delta z)] \tag{1}$$

where A_0 represents the amplitude of the interference signal, $\phi$is the phase difference between the sample and the reference surface, and Δz is the optical path difference between the sample and the reference surface.

In the presence of the birefringence in the sample, the polarization of the signal reflected from the sample is modified, and therefore (1) is only valid for the component of the polarization of the reflected sample signal which has the same polarization as the reference signal. To accommodate the effect of the birefringence, a birefringence dependent factor should be introduced in (1), which can now be written as [22]

$$A_{ref_1}(\Delta z) = A_{0_{ref_1}}(\Delta z)\cos[\phi(\Delta z)]\cos[\delta(z)] \tag{2}$$

Equation 2 represents the interference signal where the reflected sample signal has the same polarization as the reference (ref_1) signal polarization and δz is the sample retardance. For a homogenous sample where $\delta z = 0$, (2) becomes the same as (1) but for a birefringent sample where δz is non-zero, the intensity of the acquired image along the axial direction of the sample is modulated. This leads to loss of signal from some areas of the sample images and this lost signal can only be retrieved if the sample signal interferes with another reference signal which has polarization orthogonal (ref_2) to the input signal polarization. The interfered signal, in this case, can be represented as [22]

$$A_{ref_2}(\Delta z) = A_{0_{ref_2}}(\Delta z)\cos[\phi(\Delta z)]\sin[\delta(z)] \tag{3}$$

The effect of the sample birefringence can be minimized if two orthogonal reference signals are used and in this case, the total signal measured at the detector is the sum of the interference signals represented by (2) and (3). In our work, we have used this approach to minimize the effect of the sample birefringence where we have used a Faraday rotator to obtain a reference signal with polarization orthogonal to the input signal. The two reference signals with polarization orthogonal to each other were combined and used as a reference signal.

The schematic diagram of the polarization-independent optical coherence tomography (PI-OCT) system is shown in Fig. 1. The system was based on a commercially available swept-source OCT engine (Axsun Technologies, USA), with a central wavelength of 1310 nm, a bandwidth of 130 nm, and a repetition rate of 100 kHz. The output power of the laser source was 24 mW.

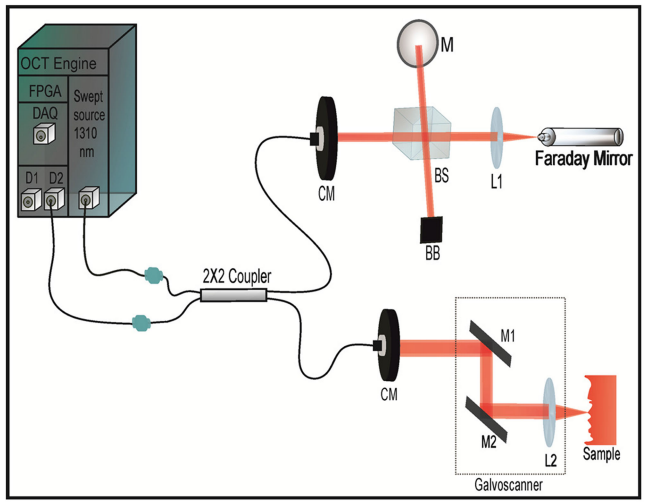

Fig. 1. Schematic diagram of the polarization insensitive OCT system. Collimator (CM), Mirror (M), Lens (L), Beam Splitter (BS), Beam Blocker (BB), Detector (D).

In this system, the output of the light source was split into the reference arm and sample arm through a fiber coupler at a split ratio of 50/50 in the reference arm.

The light was further divided into two parts using a 50/50 beam splitter (BS012, Thorlabs, Inc.), one part was directed towards a gold coated mirror placed on a translational stage and another towards a Faraday mirror (F-FRM-1-NT-FA, Newport Corporation, California), to obtain orthogonally polarized light from the reference arm. The gold-coated mirror and the Faraday mirror were aligned to provide equal amplitude at the detector. The optical path length between the Faraday mirror and the gold mirror was set to zero which provided polarization artifact-free images of the sample composed of two overlapping orthogonally polarized sample images. In the sample arm, two-axis Galvoscanner was used for scanning the beam over the sample in the X and Y direction. The reflected light from the reference arm and the sample arm was directed by the coupler towards an integrated photodiode in the OCT engine. The detected signal from the detector was digitized by a 12 bit, 500 MS/s onboard digitizer. The collected data from the digitizer was transferred to a built-in field-programmable gate array (FPGA) module, which processed the received data which involved applying a Hamming window on the acquired spectrum and a subsequent inverse Fourier transform. 2500 axial scans were collected to form a B-scan of the sample and transferred to the host computer over an Ethernet cable.

On the host computer, a custom-designed LabView software was used to collect the imaging data from the OCT engine. The LabView software only acted as an interface between the OCT engine and host workstation and was responsible for the acquisition of the images from the FPGA module, displaying the images on the screen and then saving them to the hard drive on the host workstation.

III. Results

The developed system has a lateral resolution, axial resolution, and imaging range of 5.1 μm, 5 μm, and 5.5 mm

respectively. To check the performance of the polarization insensitive OCT system, we measured the effect of the sample arm polarization change on the measured intensity of the axial point spread function (PSF). In order to achieve this, we put a mirror in the sample arm as a sample. The gold mirror in the reference arm was translated to a location such that the two peaks in the axial scan corresponding to the interference between the sample mirror/gold mirror and the sample mirror/Faraday mirror were obtained. Next by twisting the fiber in the sample arm, the polarization of the sample arm was matched to the polarization from the gold mirror. Under this condition, one can see from Fig. 2(a) that the peak in the axial scan corresponding to the interference between the gold mirror and the sample mirror is maximum whereas the peak corresponding to the interference between the Faraday mirror and the sample mirror is small. Further, we changed the polarization of the sample arm again in such a way that now the polarization of the sample arm matched to the polarization of the signal from the Faraday mirror, and under this condition, it can be seen from Fig. 2(b) that the peak corresponding to the Faraday mirror is maximum and the peak corresponding the gold mirror is small. However, the sum of the two peaks (Fig 2(c)) was approximately constant over the time period of 20 seconds when the polarization of the reference arm was changed from matching to the gold mirror to matching to the Faraday mirror. This experiment demonstrates that the two reference signals are orthogonal to each other and the loss in the sample signal intensity because of the change in the polarization in the sample arm can be effectively retrieved using two mutually orthogonal reference signals.

To demonstrate the suitability of our approach for biological samples, we imaged the nail bed of a healthy volunteer. No approval from the Ethics committee is required for such an imaging procedure. The nail bed is a well know birefringent tissue and thus is a suitable sample to demonstrate the working of our approach. For the imaging of the nail bed, the optical path difference between the gold mirror and the Faraday mirror was adjusted to zero using the translational stage such that the two images of the nail bed corresponding to the two reference surfaces overlapped each other. In Fig. 3 we show the images of the nail bed acquired under different conditions. In Fig. 3(a), an image of the nail bed is shown when the reference signal from the Faraday mirror was blocked. One can see the alternating bright and dark bands in the image which appear because of the birefringence in the tissue. In Fig. 3(b), we show the image of the nail bed when the reference signal from the gold mirror was blocked. Now again the alternating intensity bands in the image can be seen but these intensity variations are complementary to the variations in the image shown in Fig. 3(a). In Fig. 3(c), we show the image of the nail bed when both the reference signals are present. It can be seen from Fig. 3(c) that when both the reference signals are present, the alternating intensity variations in the image are minimized demonstrating that the use of two orthogonal reference signals can minimize the sample birefringence or sample arm polarization associated image artifacts. There was some additional fixed pattern noise as seen in Fig. 3(b) and Fig. 3(c), coming from the multiple optical interfaces within

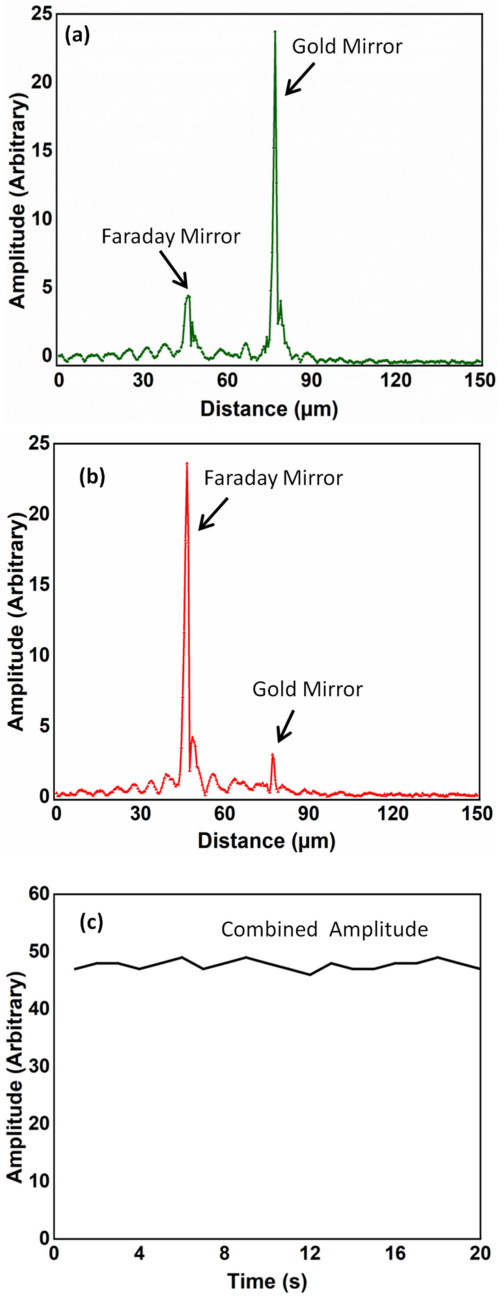

Fig. 2. Axial scan of a mirror as a sample corresponding to the sample polarization matched to the reference signal from (a) gold mirror and (b) Faraday mirror. The combined amplitude (c) of the PSF peaks when both the reference signals are present.

the Faraday mirror which could not be fully removed as we did not perform balanced detection.

We also performed ex vivo swine esophagus imaging which has more clinical relevance. In Fig. 4 we show the images of the esophagus tissue with PI-OCT system.

In Fig. 4(a), the image of the esophagus acquired without the reference signal from the Faraday Mirror is shown. The image of the esophagus with the reference signal from the gold mirror blocked is shown in Fig. 4(b). It can be seen from the image

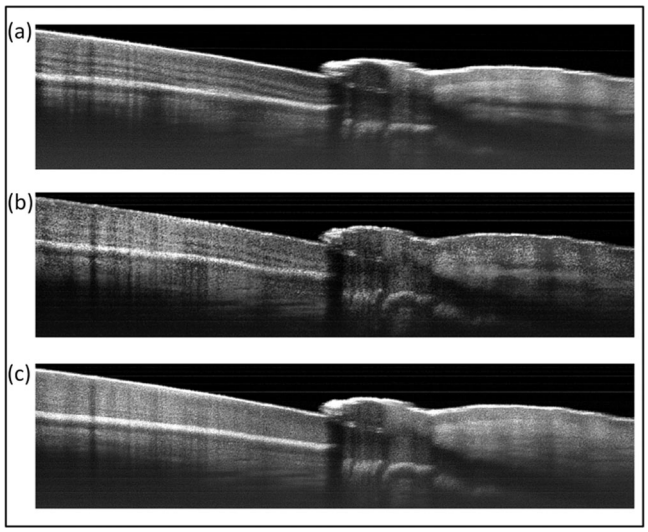

Fig. 3. Image of a nail bed when the reference signal is blocked from the (a) Faraday mirror and (b) from the gold mirror. Image of the nail bed when both the reference signals are present is shown in (c).

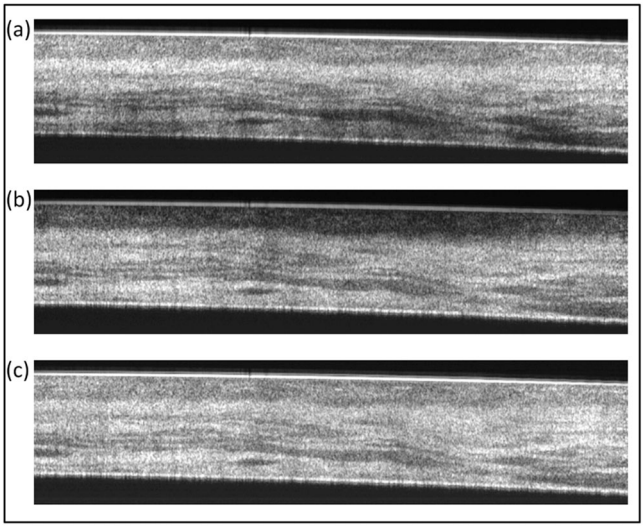

Fig. 4. Image of the esophagus when the reference signal is blocked from the (a) Faraday mirror and (b) from the gold mirror. Image of the esophagus when both the reference signals are present is shown in (c).

in Fig. 4(b), that the top esophagus layer appears dark which suggests that this layer has minimal birefringence. At the same time, the lower part of the esophagus is brighter in the image corresponding to the Faraday mirror suggesting higher birefringence or scattering dependent polarization change. The image of the esophagus when both the orthogonal reference signals are present is shown in Fig. 4(c) and free from polarization artifacts.

IV. Conclusion

We present a simple design for a polarization-insensitive OCT system using two orthogonally polarized reference signals. Our approach enables us to mitigate the polarization-dependent image artifacts which come from a combination of the sample birefringence, scattering within the sample, and fiber movements. Unlike previous approaches [30]–[32], we can minimize the polarization-dependent image artifacts without the use of any active polarization controller. This improves the system stability allowing for faster clinical adoption. In our experiments, we have used a Faraday mirror to achieve orthogonally polarized light but the rotation angle of a Faraday mirror is wavelength dependent. If a very wide band light source is used then the polarization artifacts might not be fully compensated. However, we did not observe such artifacts in the images acquired during this work. The use of Faraday mirror in free space configuration also avoids vibration-associated polarization changes in the reference signal coming from the optical fibers. Normal laboratory vibrations do not change the orthogonality of the two reference signals in our system which provides a stable polarization artifact-free image. Our approach is compatible with both, the swept-source-based OCT systems and the camera-based OCT systems. The present approach should not be confused with PS-OCT, CP-OCT, or PD-OCT approaches which can all provide polarization artifacts free images but the strength of the current approach is in its simplicity, i.e., requirement of a single detector and free from the use of any polarization controller while providing polarization artifact-free sample images. We believe that the present approach will aid in faster adoption of the OCT technique in the clinic where polarization-dependent artifacts are common because of the sample properties or the optical fiber movements.

References

[1] D. Huang *et al.*, "Optical coherence tomography," *Science*, vol. 254, 1991, Art. no. 1178.
[2] C. Dion, K. Singh, T. Ozaki, M. R. Lesk, and S. Costantino, "Analysis of pulsatile retinal movements by spectral-domain low-coherence interferometry: Influence of age and glaucoma on the pulse wave," *PLoS One*, vol. 8, 2013, Art. no. e54207.
[3] M. Pircher, C. K. Hitzenberger, and U. Schmidt-Erfurth, "Polarization sensitive optical coherence tomography in the human eye," *Prog. Retinal Eye Res.*, vol. 30, pp. 431–451, 2011.
[4] P. H. Tomlins and R. K. Wang, "Theory, developments and applications of optical coherence tomography," *J. Phys. D: Appl. Phys.*, vol. 38, 2005, Art. no. 2519.
[5] G. F. Schmid, B. L. Petrig, C. E. Riva, E. Logean, and R. Wälti, "Measurement of eye length and eye shape by optical low coherence reflectometry," *Int. Ophthalmol.*, vol. 23, pp. 317–320, 2001.
[6] D. Huang, J. Wang, C. P. Lin, C. A. Puliafito, and J. G. Fujimoto, "Micron-resolution ranging of cornea anterior chamber by optical reflectometry," *Lasers Surg. Med.*, vol. 11, pp. 419–425, 1991.
[7] M. Wojtkowski, R. Leitgeb, A. Kowalczyk, T. Bajraszewski, and A. F. Fercher, "In vivo human retinal imaging by Fourier domain optical coherence tomography," *J. Biomed. Opt.*, vol. 7, pp. 457–463, 2002.
[8] A. F. Fercher, C. K. Hitzenberger, G. Kamp, and S. Y. El-Zaiat, "Measurement of intraocular distances by backscattering spectral interferometry," *Opt. Commun.*, vol. 117, pp. 43–48, 1995.
[9] M. A. Choma, K. Hsu, and J. A. Izatt, "Swept source optical coherence tomography using an all-fiber 1300-nm ring laser source," *J. Biomed. Opt.*, vol. 10, 2005, Art. no. 044009.
[10] A. Y. Alibhai, C. Or, and A. J. Witkin, "Swept source optical coherence tomography: A review," *Curr. Ophthalmol. Rep.*, vol. 6, pp. 7–16, 2018.
[11] K. Singh *et al.*, "Pulsatile movement of the optic nerve head and the peripapillary retina in normal subjects and in glaucoma," *Invest. Ophthalmol. Vis. Sci.*, vol. 53, pp. 7819–7824, 2012.
[12] M. Ibne Mokbul, "Optical coherence tomography: Basic concepts and applications in neuroscience research," *J. Med. Eng.*, vol. 2017, 2017, Art. no. 3409327.

[13] Y. Wang, S. Liu, S. Lou, W. Zhang, H. Cai, and X. Chen, "Application of optical coherence tomography in clinical diagnosis," *J. X-Ray Sci. Technol.*, vol. 27, pp. 995–1006, 2019.

[14] J. Golde *et al.*, "Detection of carious lesions utilizing depolarization imaging by polarization sensitive optical coherence tomography," *J. Biomed. Opt.*, vol. 23, 2018, Art. no. 071203.

[15] M. Tajmirriahi, Z. Amini, A. Hamidi, A. Zam, and H. Rabbani, "Modeling of retinal optical coherence tomography based on stochastic differential equations: Application to denoising," *IEEE Trans. Med. Imag.*, vol. 40, no. 8, pp. 2129–2141, Aug. 2021.

[16] M. L. Olender, L. S. Athanasiou, M. José, E. Ben-Assa, F. R. Nezami, and E. R. Edelman, "A mechanical approach for smooth surface fitting to delineate vessel walls in optical coherence tomography images," *IEEE Trans. Med. Imag.*, vol. 38, no. 6, pp. 1384–1397, Jun. 2019.

[17] H. Lin, Z. Zhang, D. Markl, J. A. Zeitler, and Y. Shen, "A review of the applications of OCT for analysing pharmaceutical film coatings," *Appl. Sci.*, vol. 8, 2018, Art. no. 2700.

[18] M. Nioi, P. E. Napoli, S. M. Mayerson, M. Fossarello, and E. d'Aloja, "Optical coherence tomography in forensic sciences: A review of the literature," *Forensic Sci. Med. Pathol.*, vol. 15, pp. 445–452, 2019.

[19] A. I. Koponen and S. Haavisto, "Analysis of industry-related flows by optical coherence Tomography—A review," *KONA Powder Part. J.*, vol. 37, pp. 42–63, 2020.

[20] S. Sharma, G. Hartl, S. K. Naveed, K. Blessing, G. Sharma, and K. Singh, "Input polarization-independent polarization-sensitive optical coherence tomography using a depolarizer," *Rev. Sci. Instrum.*, vol. 91, 2020, Art. no. 043706.

[21] B. Baumann, "Polarization sensitive optical coherence tomography: A review of technology and applications," *Appl. Sci.*, vol. 7, 2017, Art. no. 474.

[22] J. F. De Boer, C. K. Hitzenberger, and Y. Yasuno, "Polarization sensitive optical coherence tomography–A review," *Biomed. Opt. Exp.*, vol. 8, pp. 1838–1873, 2017.

[23] K. Blessing, J. Schirmer, G. Sharma, and K. Singh, "Novel input polarisation independent endoscopic cross-polarised optical coherence tomography probe," *J. Biophoton.*, vol. 13, 2020, Art. no. e202000134.

[24] K. Blessing, J. Schirmer, A. Parmar, and K. Singh, "Depth encoded input polarisation independent swept source cross-polarised optical coherence tomography probe," *J. Phys. D: Appl. Phys.*, vol. 54, 2021, Art. no. 305401.

[25] V. Gelikonov *et al.*, "Cross-polarization optical coherence tomography with active maintenance of the circular polarization of a sounding wave in a common path system," *Radiophys. Quantum Electron.*, vol. 60, pp. 897–911, 2018.

[26] K. S. Yashin *et al.*, "Quantitative nontumorous and tumorous human brain tissue assessment using microstructural co-and cross-polarized optical coherence tomography," *Sci. Rep.*, vol. 9, pp. 1–12, 2019.

[27] X. Yao, Y. Gan, Y. Ling, C. C. Marboe, and C. P. Hendon, "Multicontrast endomyocardial imaging by single-channel high-resolution cross-polarization optical coherence tomography," *J. Biophoton.*, vol. 11, 2018, Art. no. e201700204.

[28] V. Gelikonov and G. Gelikonov, "New approach to cross-polarized optical coherence tomography based on orthogonal arbitrarily polarized modes," *Laser Phys. Lett.*, vol. 3, 2006, Art. no. 445.

[29] K. Blessing, J. Schirmer, G. Sharma, and K. Singh, "Novel input polarisation independent endoscopic cross polarised optical coherence tomography probe," *J. Biophoton.*, vol. 13, 2020, Art. no. e202000134.

[30] B. J. Vakoc, S. H. Yun, G. J. Tearney, and B. E. Bouma, "Elimination of depth degeneracy in optical frequency-domain imaging through polarization-based optical demodulation," *Opt. Lett.*, vol. 31, pp. 362–364, Feb. 2006.

[31] A. M. Lee, H. Pahlevaninezhad, V. X. Yang, S. Lam, C. MacAulay, and P. Lane, "Fiber-optic polarization diversity detection for rotary probe optical coherence tomography," *Opt. Lett.*, vol. 39, pp. 3638–3641, 2014.

[32] D. O. Otuya, G. Sharma, G. J. Tearney, and K. Singh, "All fiber polarization insensitive detection for spectrometer based optical coherence tomography using optical switch," *OSA Continuum*, vol. 2, pp. 3465–3469, 2019.